Article ID: 1005 - 9784(2006)05 - 0577 - 07

Numerical simulation for influence of excavation and blasting vibration on stability of mined-out area①

XU Guo-yuan(徐国元), YAN Chang-bin(闫长斌)
(School of Resources and Safety Engineering, Central South University, Changsha 410083, China)

Abstract: Dynamic analysis steps and general flow of fast lagrangian analysis of continua in 3 dimensions (FLAC3D) were discussed. Numerical simulation for influence of excavation and blasting vibration on stability of mined-out area was carried out with FLAC3D. The whole analytical process was divided into two steps, including the static analysis and the dynamic analysis which were used to simulate the influence of excavation process and blasting vibration respectively. The results show that the shape of right upper boundary is extremely irregular after excavation, and stress concentration occurs at many places and higher tensile stress appears. The maximum tensile stress is higher than the tensile strength of rock mass, and surrounding rock of right roof will be damaged with tension fracture. The maximum displacement of surrounding rock is 4.75 mm after excavation. However, the maximum displacement increases to 5.47 mm after the blasting dynamic load is applied. And the covering area of plastic zones expands obviously, especially at the foot of right upper slope. The analytical results are in basic accordance with the observed results on the whole. Damage and disturbance on surrounding rock to some degree are caused by excavation, while blasting dynamic load increases the possibility of occurrence of dynamic instability and destruction further. So the effective supporting and vibration reducing measures should be taken during mining.

Key words: mined-out area; excavation process; blasting vibration; stability; numerical simulation; FLAC3D
CLC number: TD235+.3; TD235.1 **Document code**: A

1 INTRODUCTION

Excavation and dynamic stability of underground chambers is one of the hotspots in rock mechanics and engineering research all the while, especially in hydroelectric underground houses and mined-out areas in mining, laneways, etc. Martin et al[1-2] studied the law of stress, displacement and stability of chambers after excavation, and got some significant conclusions. Chern et al[3-4] discussed the stability of underground chambers affected by earthquake and blasting vibration respectively. However, instability or damage of underground chambers is caused by excavation and dynamic load together. So the influence of two factors on stability of underground chambers should be considered at the same time.

Changba lead-zinc mine is located at Huangzhu town, Cheng county, Gansu province. It is one of the super large-scale lead-zinc deposits. Since later 80's of the twentieth century, local crazy civil mining has caused giant economic loss to the mine. Millions of square meters unsettled mined-out areas group left by civil mining threatens the normal mining seriously. Geologic hazards induced by mined-out areas group occur frequently, and catastrophic accidents are caused to happen continuously[5-7]. So Changba lead-zinc mine has been forced to turn to underground ahead of schedule. The trend that complex mined-out areas come to dynamic instability because of later mining blasting operation is obvious day by day. In order to ensure mining safety of transition layer, blasting seismic effect test in situ and analysis have been carried out, and relatively accurate basic data are obtained. In order to study the process and mechanism that dynamic instability of complex mined-out areas under blasting vibration load, three dimensional numerical simulations were carried out with fast lagrangian analysis of continua in 3 dimension (FLAC3D) based on test in situ. During the numerical simulation, influence on mined-out areas stability by excavation process and blasting vibration is considered at the same time.

2 DYNAMIC ANALYSIS BY FLAC3D

FLAC3D is a three-dimensional explicit finite-difference program for engineering mechanics computation. It was developed by Itasca Consulting

① **Foundation item**: Project (50490272) supported by the National Natural Science Foundation of China; project(NCET-05-0687) supported by Program for New Century Excellent Talents; project (040109) supported by the Doctor Degree Paper Innovation Engineering of Central South University
Received date: 2005 - 12 - 28; **Accepted date**: 2006 - 03 - 25
Correspondence: YAN Chang-bin, Doctoral candidate; Tel: +86-731-8832419, 13787120798; E-mail: yanchangbin_2001@163.com

Group Inc. FLAC3D extends the analysis capability of FLAC into three dimensions, simulating the behavior of three-dimensional structures of soil, rock or other materials that undergo plastic flow when their yield limits are reached, which provided an ideal analytical tool for settling three-dimensional computational problems in geotechnical engineering fields[8-11].

Dynamic analysis must be carried out after excavation computation has been finished. Static computation is the precondition of dynamic analysis. FLAC3D analysis can be divided into the following steps:

1) Defining computational range, modeling and plotting;

2) Choosing computational mode, defining constitutive model and physical mechanical parameters of materials;

3) Defining initial condition and boundary conditions;

4) Getting initial balance state, which is field stress state before excavation;

5) Carrying out engineering excavation, static computational analysis, and getting static results;

6) Checking the static results, if they are satisfying, then dynamic boundary condition and damping are set up; otherwise, returning to 1), redefining conditions and calculating again, until satisfactory results are gotten;

7) Applying dynamic loads, carrying out dynamic analysis, and getting dynamic results. General computational flow is shown in Fig. 1.

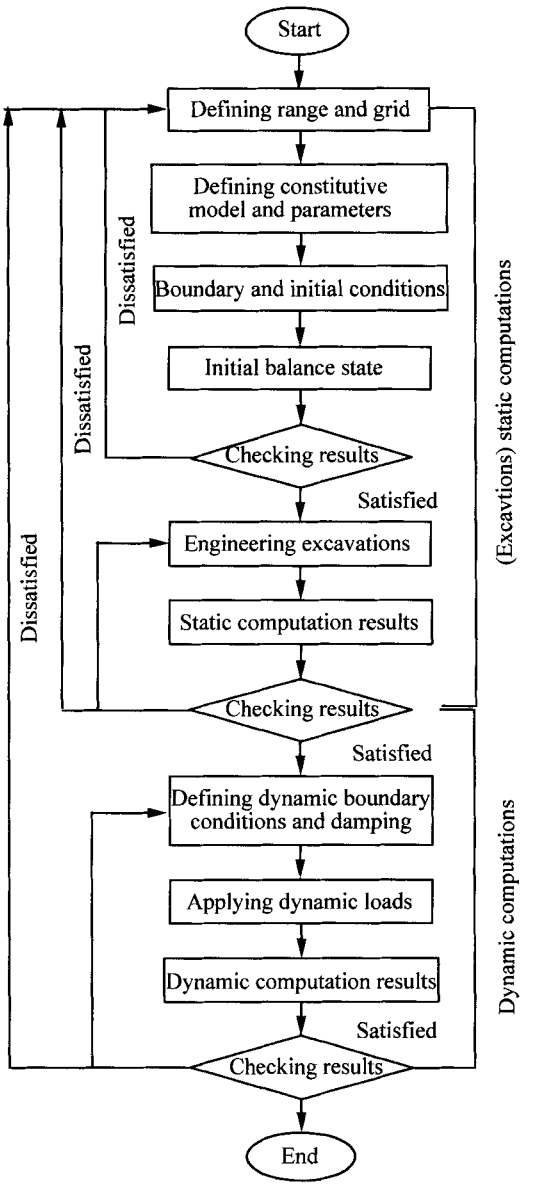

Fig. 1 General flow chart of FLAC3D analysis

3 GENERAL ENGINEERING ASPECT

3.1 Geologic features

The mine is located at the north of Wujia Mountain anticline and the south of hypo-level Wangjia Mountain syncline. The stratum belongs to Devonian, middle series, Xihanshui Group, the second subgroup (D_2^{2-2}) and the third subgroup (D_2^{2-3}). According to mineral component and structural features, the stratum is divided into nine layers: quartz schist, biotite schist, biotite quartz schist, hoar middle crystal granules and interring calcite biotite schist, mica banding crystalline limestone and calcite quartz schist, white granule dolomite, quartz biotite schist and gray medium-grained crystalline limestone.

3.2 Deposit features

There are 51 lead-zinc ore bodies big or small in the mine field. Where the scale of ore bodies Ⅰ and Ⅱ is the biggest, they are key ore bodies. The shape of ore body Ⅰ is complicated relatively. It is an irregular layer, nervational, cystoids body. Ore body Ⅰ is mainly distributed between line 33 and line 69, and its length is 680 m. Its height mark is in the range of 1 630 - 860 m. The shape of ore body Ⅱ is rather regular, and like layer. The boundary line between surrounding rock is rather clear. It is mainly distributed between line 33 and line 49, and its length is 380 m. Its height mark is in the range of 1 500 - 910 m. Ore body Ⅱ is mostly of massive ore, which has higher compression strength and is rather stable. The crack is not fully grown. The surrounding rock of upper and bottom is made up of biotite, whose joints and crack are not relatively fully grown and compression strength is higher and is generally stable.

4 COMPUTATIONAL ANALYSIS

4.1 Computational model

4.1.1 Model dimension

According to mined-out area exploration re-

sults, there is large-scale civil mining mined-out area in ore body Ⅱ, and different mined-out areas have been connected and joined to one big body. Therefore, ore body Ⅱ and its surrounding rock are chosen as the computational domain. Its size is 120 m×180 m ×125 m. The mined-out area is located at the center of the domain, as shown in Fig. 2. The mined-out area is 24 m high, and its bottom is wider than top. It is 36 m wide at bottom and 11 m wide at top, 32 m extending along ore body. The upper boundary of model is land surface, and the distance between the lower boundary of model and bottom of mined-out area is 70 m. The distance of left wall and right wall is 90 m and 60 m respectively, 88 m is along ore body(y direction). According to Saint-Venant principle, the model size satisfies the requirement of computational accuracy.

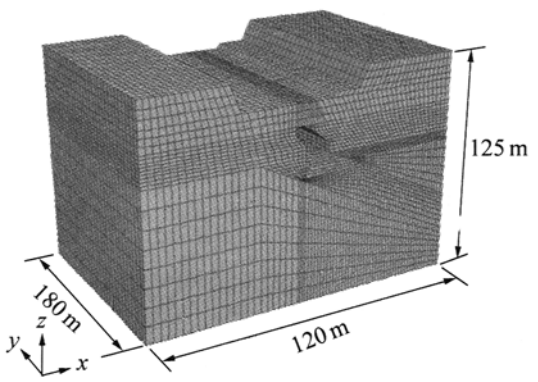

Fig. 2 FLAC3D model after excavation

4.1.2 Establishing numerical model

The FLAC3D grid of model after excavation is shown in Fig. 2. There are 70 200 elements and 75 733 nodes in the model; according to parameters of lithology, the model can be divided into three zones, which are mined-out area, ore body and surrounding rock. The model size is the same as actual size. Shape and position of mined-out area are defined by referring exploration results. According to investigation in situ, rock category within the model is relatively simple. Surrounding rock is rather intact, and there are not faults and obvious cranny. So the rock mass can be divided into two big classes, surrounding rock and ore. The surrounding rock of upper and bottom is biotite, and the ore is lead-zinc.

4.1.3 Initial condition and boundary condition

Initial stress field: the buried depth of mined-out area is comparatively shallow. Tectonic stress in the mine field is not obvious. So ground stress in situ is not measured. In initial stress field is only gravity stress field is taken into account. According to principles of elasticity, vertical stress is given by $\sigma_v=\gamma H$, and horizontal stress is given by $\sigma_h=K\sigma_v$, where γ is the unit weight, H is the buried depth, lateral pressure coefficient $K=\mu/(1-\mu)$, μ is the poisson ratio.

Boundary condition: displacement boundary condition is used, that is to say, the left and right (x direction) boundary, the frontal and back (y direction) boundary and bottom boundary are all applied displacement constraint condition. The upper boundary is free.

4.2 Physical mechanical parameter of rock mass

The physical mechanical parameters of rock mass required in the computation have been gotten by discounting the physical mechanical parameters of rock obtained through lab test[12], and the concrete parameters are listed in Table 1.

Table 1 Physical mechanical parameters of rock mass from Changba lead-zinc mine

Rock type	Compression strength/ kPa	Tensile strength/ MPa	Deformation modulus/ GPa	Cohesion/ kPa
Lead-zinc ore	7.716 1	205.2	13.22	629.2
Biotite schist	8.569 3	245.9	12.98	725.8

Rock type	Angle of internal friction/ (°)	Poisson ratio	Density/ ($t \cdot m^{-3}$)
Lead-zinc ore	71.47	0.26	2.721
Biotite schist	70.77	0.22	2.723

4.3 Numerical scheme

In order to study secondary state of stress and variance of displacement after excavation, find out the law of redistribution of secondary state of stress under blasting vibration and further variance of displacement, and confirm the main hazards and degree of damage to mined-out area by excavation and blasting vibration, the whole analysis is divided into two steps which are static computation and dynamic computation. And there are two computational schemes:

1) In natural gravity stress field, the computation and analysis of excavation process;

2) Dynamic analysis after dynamic load is applied based on static analysis.

Mohr-Coulomb criterion, that is elastic-plastic model, is applied in the computation. And macro-strain computational mode is selected.

5 BLASTING VIBRATION INPUT

5.1 Time history curve of velocity

In order to get the first hand data, blasting vibration test effect in situ has been finished in Changba lead-zinc mine. Vibration velocity was selected as the physical parameter during test, and test instruments were IDTS3850 with two channels

and, three channels blasting vibration recorders which were developed by Chengdu Zhongke Dynamic Instrument Inc. Transducers were SCD-Z vertical and SCD-P horizontal velocity transducers.

The vibration velocity in the calculation came from driving blasting seismic effect test of some laneway in situ, which is shown in Fig. 3. Its main parameters were as follows: its basic frequency is 12.28 Hz, the lasting time is 5.15 s, and the maximum amplitude is 0.460 9 m/s.

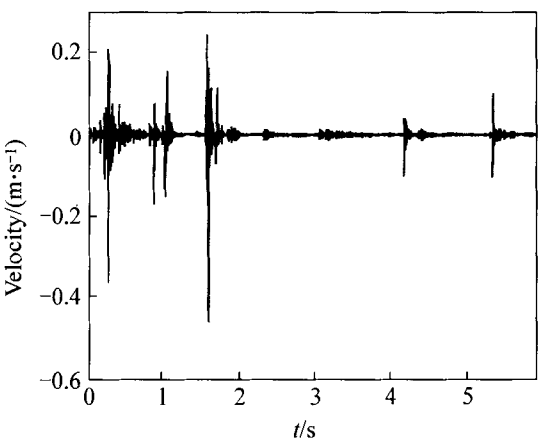

Fig. 3 Velocity series of blasting vibration

5.2 Applying blasting dynamic

In FLAC3D dynamic computation and analysis, dynamic loads input to the model can be one of four modes, which are acceleration, velocity, displacement and stress. If the viscid boundary condition is used, then dynamic loads input must be velocity[9, 13]. What is more, the testing data is also vibration velocity of particle, so the vibration velocity was selected as dynamic loads input. Since testing data was all from floor of mined-out areas or laneways, blasting dynamic loads were applied to the floor of mined-out area. The dynamic loads propagate along negative direction of z axes.

6 ANALYSIS OF SIMULATION RESULTS

The whole computational process is made up of two parts, which are static(excavation)analysis and dynamic analysis. Static computation is the precondition. Dynamic computation must be carried out based on static analysis. The excavation of whole mined-out area is divided into eight steps during the static analysis, and every step of excavation is 4 m along y direction. The balance state is reached by computing after each excavation step is finished, until the excavation of whole mined-out area is completed. In FLAC3D, when the ratio of the maximum unbalanced force for all the grid points in the model falls below 10^{-5}, then the balance state occurs and the calculation will stop. The value of dynamic loads is put on the floor of mined-out area through table format when dynamic computation is carried out, and then dynamic analytical results are gotten.

6.1 Analysis of stress

The distributions of maximum principle stress of excavation and dynamic loads are shown in Figs. 4 and 5 respectively. The variance of maximum principle stress, maximum displacement and area of plastic zones with steps of calculation are listed in Table 2. It can be found out that the boundary shape of mined-out area is extremely irregular, and has basically formed "crag" situation. Stress redistribution has taken place after excavation is finished, and stress concentration is relatively obvious at irregular boundary and corners. Higher tensile stress occurs at right above the mined-out area and floor, and it extends to the foot of right slope. From Table 2, the value of maximum tensile stress is 276.2 kPa after excavation of first step at right roof and floor. It is higher than the value of tensile strength of rock mass which is 205.2 kPa, and surrounding rock will be damaged with tension fracture. The maximum tensile stress is higher than the tensile strength of rock mass during the whole excavation process all the while, and its scope increases gradually. So almost all the right upper surrounding rock and most of floor will be destructed with tensile fracture, which can be seen in Fig. 4. There is still higher tensile stress concentration, though it is not obvious when floor

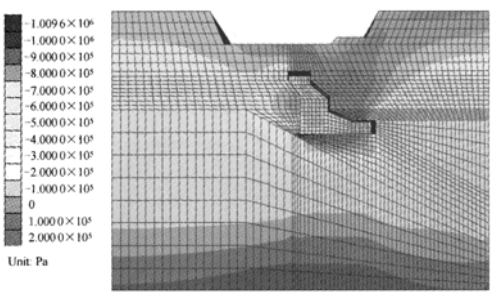

Fig. 4 Distribution of maximum principle stress after excavation

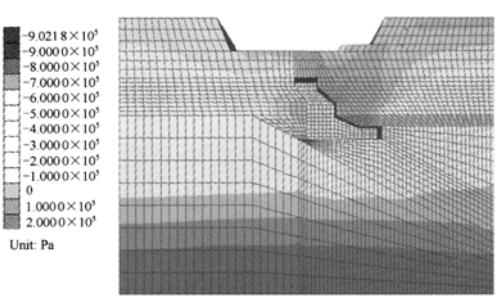

Fig. 5 Distribution of maximum principle stress under dynamic loadings

after dynamic loads are applied. However the maximum tensile stress is also higher than the tensile strength of rock mass. So the effective supporting measures and vibration reducing measures should be taken to prevent instability and subsiding of surrounding rock of right roof and floor.

Table 2 Variance of maximum principle stress, maximum displacement and area of plastic zones with steps of calculation

Steps of calculation	Maximum principle stress/kPa	Maximum displacement/mm	Area of plastic zones/m²
1st step of excavation	276.2	0.84	40
2nd step of excavation	346.5	1.32	68
3rd step of excavation	276.1	1.77	88
4th step of excavation	217.3	2.28	124
5th step of excavation	206.4	2.95	140
6th step of excavation	206.7	3.57	152
7th step of excavation	206.4	4.16	168
8th step of excavation	220.5	4.75	182
Applying dynamic loads	208.2	5.47	292

6.2 Analysis of displacement

The distributions of displacement of excavation and dynamic loads are shown in Figs. 6 and 7 respectively. It can be found from Fig. 6, Fig. 7 and Table 2 that the displacement increases gradually during excavation process of mined-out area. The maximum displacement of surrounding rock is 4.75 mm after excavation is finished, and the maximum displacement occurs at the right upper boundary. There is also higher displacement at the floor and within the foot of right slope. The maximum displacement comes up to 5.47 mm after dynamic loads are applied, and its distribution scope has changed. The maximum displacement also occurs at the right upper boundary under dynamic loads, but its value is higher than the value of maximum displacement after excavation. However, the distribution scope at floor becomes small. It is shown that not only the value of maximum displacement increases, but also the distribution shape and scope change after dynamic loads are applied. The variance law of displacement in z direction of some monitoring point at the foot of right slope with calculating steps is shown in Fig. 8. From Fig. 8, it can be seen that the displacement of this monitoring point of excavation phase and dynamic load phase is 3.75 mm and 4.69 mm respectively. During dynamic loads phase, displacement curve turns to upward slowly when calculating step is over 2.4×10^5, which results from comeback of elastic displacement. The influence of underground excavation and blasting vibration on the slope must be considered, because mining production of opening up and underground operates at the same time. To insure the safety of production, displacement monitoring in situ has been carried out at the foot of right slope with multi-points displacement meters. The value of monitoring displacement is 5.13 mm, which is higher than the computational value 4.69 mm. Its main reasons are that monitoring displacement is the result of repeating excavation and blasting vibration, while the computational value is only caused by part of excavation and once blasting vibration.

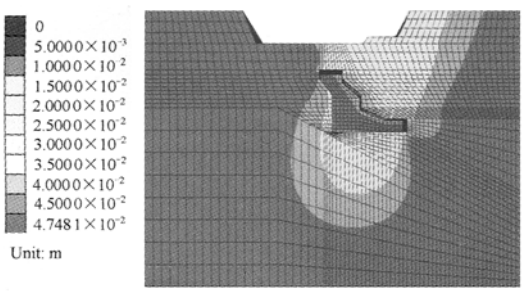

Fig. 6 Distribution of displacement after excavation

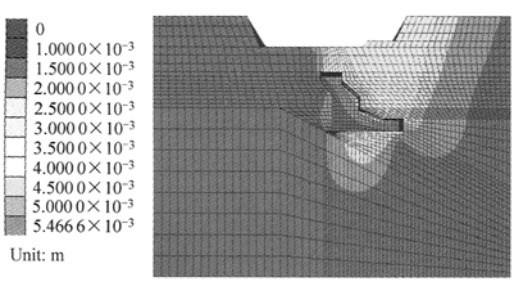

Fig. 7 Distribution of displacement under dynamic loadings

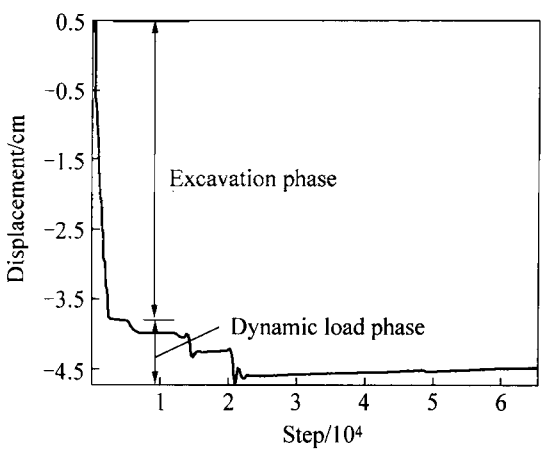

Fig. 8 Law of displacement in z direction of some monitoring points

6.3 Analysis of plastic zones

The variant law of plastic zones area with different computational conditions under excavation and blasting vibration is shown in Fig. 9. The position distribution of plastic zone under different

computational conditions is shown in Fig. 10. From Fig. 9, it can be seen that the distribution area of plastic zone increases gradually with the increase of steps of excavation. However, the area of plastic zone increases suddenly after dynamic loads are applied. Therefore, blasting vibration causes important influence on expansion of plastic zones. It is found from Fig. 10 that the distribution range of plastic zones is rather wide, and most of them occur at right upper boundary surrounding rock and floor. The distribution of plastic zones extends gradually with the advance of excavation process and blasting vibration. The plastic zones begin to appear at the foot of right slope after the eighth step of excavation, or the whole mined-out area is finished. The distribution scope of plastic zones expands obviously after dynamic loads are applied, and the plastic zones appear at foots of both left and right side slope.

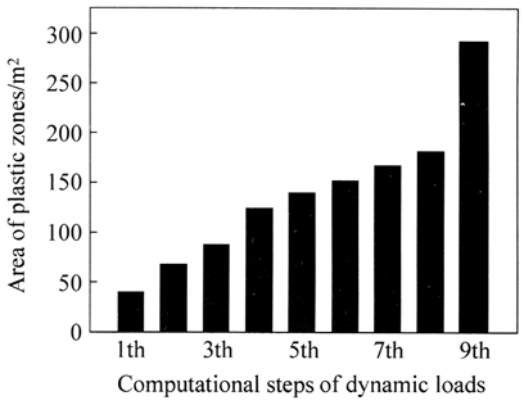

Fig. 9 Variant law of plastic zones area under dynamic loads

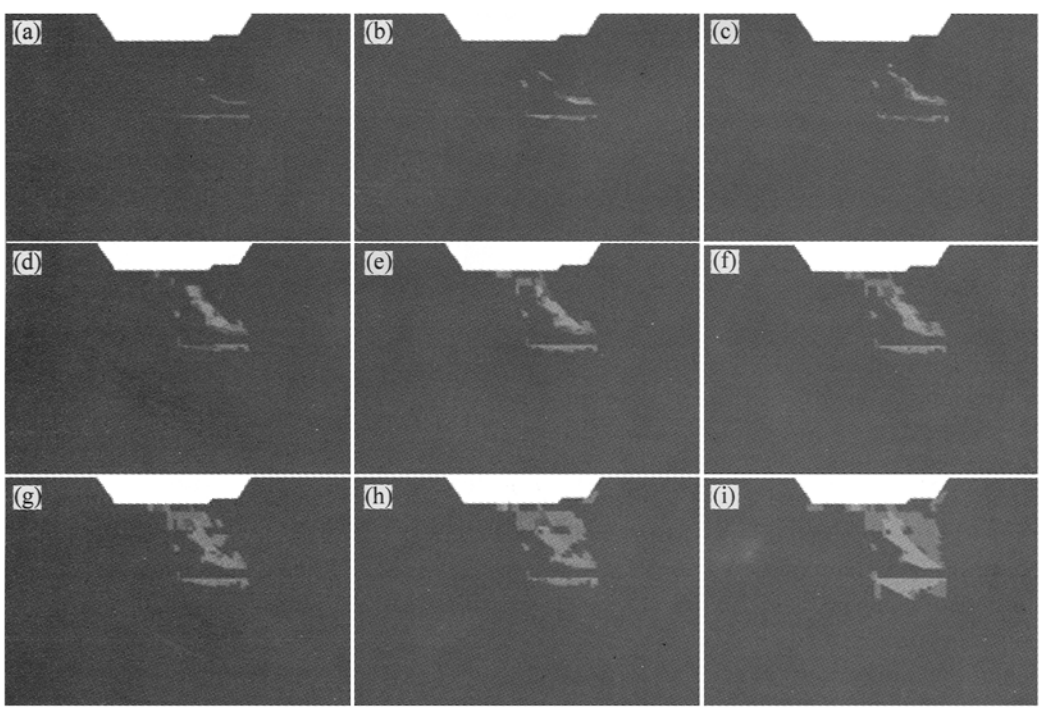

Fig. 10 Position distribution of plastic zone under different computational conditions
(a)—1st step of excavation; (b)—2nd step of excavation; (c)—3rd step of excavation; (d)—4th step of excavation; (e)—5th step of excavation; (f)—6th step of excavation; (g)—7th step of excavation; (h)—8th step of excavation; (i)—Applying dynamic loads

7 CONCLUSIONS

1) The shape of right upper boundary is extremely irregular, and has basically formed "crag" situation after excavation of mined-out area. Stress concentration occurs at many places and higher tensile stress appears. The maximum tensile stress of surrounding rock is higher than the tensile strength of rock mass during the whole excavation process, and almost all the right upper surrounding rock and most of floor will be destructed with tensile fracture. The maximum tensile stress of surrounding rock is still higher than the tensile strength of rock mass after dynamic loads are applied.

2) The maximum displacement occurs at the right roof of mined-out area after excavation, and its value is 4.75 mm. However, the maximum displacement increases to 5.47 mm after dynamic loads are applied. The distributing form and scope of displacement also change because of dynamic

loads. The value of monitoring displacement at the foot of right slope is 5. 13 mm, which is higher than the computational value 4. 69 mm. Its main reasons are that monitoring displacement is the result of repeating excavation and blasting vibration.

3) The distribution scope of plastic zone is rather wide after excavation, because adjacent mined-out areas are connected to a big whole body. The area and distribution scope increase gradually with the increase of steps of excavation. The area of plastic zone increases suddenly after dynamic loads are applied, and distribution scope expands obviously.

4) The computational results and testing data all show that damage and disturbance to some degree are caused by excavation, and possibility of occurrence of dynamic instability and destruction enhances further during blasting operation. So the effective supporting and vibration reducing measures should be taken during mining, such as bolting-grouting support and multi-section millisecond short delay blasting, etc.

5) It is notable by theory and practice that the damage or instability of surrounding rock under blasting vibration usually results from cumulative dynamic damage and disturbance for many times. Blasting damage cumulative effect should be studied further.

REFERENCES

[1] Martin C D, Kaiser P K, Christiansson R. Stress, instability and design of underground excavations [J]. International Journal of Rock Mechanics and Mining Sciences, 2003, 40(7 - 8): 1027 - 1047.

[2] Hao Y H, Azzam R. The plastic zones and displacements around underground openings in rock masses containing a fault [J]. Tunneling and Underground Space Technology, 2005, 20(1): 49 - 61.

[3] Chern J C, Chang Y L, Lee H C. Seismic safety analysis of Kukuan underground power cavern [J]. Tunneling and Underground Space Technology, 2004, 19(4 - 5): 516 - 527.

[4] Singh P K. Blast vibration damage to underground coal mines from adjacent open-pit blasting [J]. International Journal of Rock Mechanics and Mining Sciences, 2002, 39(8): 959 - 973.

[5] DONG Yu-shu, XU Yu-ning. Some problems resulted from disordered mining of lead-zinc ores in Changba ore field [J]. Geology and Mineral Resource of South China, 2002(4): 23 - 27. (in Chinese)

[6] LIU Song-wei, YIN Xian-gang, CHEN Li-ming, et al. Engineering geology research and evaluation of transitional layer of Changba lead-zinc ore field Ⅱ# mine[J]. Mining Technology, 2003, 3(4): 1 - 4. (in Chinese)

[7] YUAN Ji-yu, CHEN Shuang-shi. Technical alteration and persistent development of mine after disordered mining destroy [J]. Express Information of Mining Industry, 2002(3): 10 - 12. (in Chinese)

[8] Itasca Consulting Group Inc. FLAC3D (Fast Lagrangian analysis of continua in 3 dimensions), Version 2.10, Users manual [Z]. USA: Itasca Consulting Group Inc, 2002.

[9] YANG Xin-an, HUANG Hong-wei, DING Quan-lu. FLAC program and its applications in tunnel engineering [J]. Journal of Shanghai Railway University, 1996, 17(4): 39 - 45. (in Chinese)

[10] HUANG Run-qiu, XU Qiang, TAO Lian-jin, et al. Research of process simulation and process control for geologic hazards[M]. Beijing: Science Press, 2002. (in Chinese)

[11] LI Ting-chun, LI Shu-cai, QIU Xiang-bo. Application of fast Lagrangian analysis of continua to researching on safe rock covers of Xiamen subsea tunnel [J]. Rock and Soil Mechanics, 2004, 25(6): 935 - 939. (in Chinese)

[12] YIN Xian-gang, LI Shu-lin, TANG Hai-yan, et al. The tests and studies of physical mechanical properties of the rocks from Changba lead-zinc mine [J]. Mining R & D, 2003, 23(5): 12 - 14. (in Chinese)

[13] LIU Chun-ling, QI Sheng-wen, TONG Li-qiang. Stability analysis of slope under earthquake with FLAC3D[J]. Chinese Journal of Rock Mechanics and Engineering, 2004, 23(16): 2730 - 2733. (in Chinese)

(Edited by YANG Hua)